SCIENCE CHINA
Technological Sciences

Special Topic: Chemomechanics
•Article•

August 2019 Vol.62 No.8: 1365–1374
https://doi.org/10.1007/s11431-018-9499-x

# A chemo-mechanical model for fully-coupled lithiation reaction and stress generation in viscoplastic lithiated silicon

BUREBI YiMing, JIA Zheng* & QU ShaoXing

*Key Laboratory of Soft Machines and Smart Devices of Zhejiang Province, Center for X-Mechanics, Department of Engineering Mechanics, Zhejiang University, Hangzhou 310027, China*

Received November 7, 2018; accepted March 19, 2019; published online July 11, 2019

Development of stresses in silicon (Si) anodes of lithium-ion batteries is strongly affected by its mechanical properties. Recent experiments reveal that the mechanical behavior of lithiated silicon is viscoplastic, thereby indicating that lithiation-induced mechanical stresses are dependent on the lithiation reaction rate. Experimental evidence also accumulates that the rate of lithiation reaction is conversely affected by the magnitude of mechanical stresses. These experimental observations demonstrate that lithiation reaction and stress generation in silicon anodes are fully coupled. In this work, we formulate a chemo-mechanical model considering the two-way coupling between lithiation reaction and viscoplastic deformation in silicon nanoparticle anodes. Based on the model, the position of the lithiation interface, the interface velocity, and the lithiation-induced stresses can be solved simultaneously via numerical methods. The predicted interface velocity is in line with experimental measurements reported in the literature. We demonstrate that the lithiation-induced stress field depends on the lithiation reaction through two parameters: the migration velocity and the position of the lithiation interface. We identify a stress-mitigation mechanism in viscoplastic silicon anodes: the stress-regulated lithiation reaction at the interface serves as a "brake" to reduce the interface velocity and mitigate the lithiation-induced stresses, protecting the Si nanoparticle anode from being subjected to excessive mechanical stresses.

**lithium-ion battery, lithiation-induced stress, stress-regulated lithiation, viscoplasticity**

**Citation:** Burebi Y M, Jia Z, Qu S X. A chemo-mechanical model for fully-coupled lithiation reaction and stress generation in viscoplastic lithiated silicon. Sci China Tech Sci, 2019, 62: 1365–1374, https://doi.org/10.1007/s11431-018-9499-x

## 1 Introduction

Silicon is emerging as a promising anode material for next-generation lithium-ion batteries due to its high theoretical capacity which is about ten times that of current graphite anodes [1,2]. The high theoretical capacity of silicon is attributed to its ability to host up to 3.75 lithium atoms per silicon atom upon full lithiation [3]. However, repeated insertion and extraction of a large number of lithium atoms induce excessive volume change (~300%) and thus large mechanical stresses, which may fracture the silicon anodes and the solid-electrolyte interface, causing significant permanent capacity decay [2,4–9]. Experimental evidence has accumulated that lithiation-induced stresses not only affect the mechanical integrity of the silicon anodes, but also conversely influence the lithiation kinetics. It is well known that the lithiation process of crystalline silicon proceeds with the movement of an atomically-sharp interface which separates a fully lithiated silicon phase and a pristine silicon phase [10,11]. As the interface progresses into the silicon anodes, the interface migration slows down gradually [12] and sometimes even halts before the silicon anodes are completely lithiated [13]. It has been reported by both experiments and finite element simulations that lithiation-induced stresses across the interface reduce the driving force of chemical reaction between Li and Si at the interface and thus

*Corresponding author (email: zheng.jia@zju.edu.cn)

 

result in the observed slowing and halting of interface [14–19]. Recent large-scale atomistic simulation based on reactive force field also reveals that external stresses play an important role in determining the lithiation kinetics [20]. To this end, understanding the chemo-mechanical coupling between lithiation reaction and stress generation in silicon anodes is fundamental to the advancement of Li-ion batteries.

Chemo-mechanical coupling between stress and lithiation reaction is strongly affected by mechanical properties of the silicon anodes, especially plasticity of the lithiated silicon. Sethuraman et al. [21,22] employed the wafer curvature method to experimentally measure the stress in Si thin-film electrodes as a function of lithium concentration and found the lithiated silicon deforms plastically with yielding stress about 1 GPa. Fan et al. [23] performed molecular dynamics simulation and revealed that the plastic deformation of lithiated silicon stems from the breaking of strong Si-Si covalent bonds and the continuous breaking and re-forming of weak Li-Li bonds which facilitate plastic flow. Moreover, a number of recent experiments have revealed that the nature of plasticity of amorphous $Li_xSi$ is rate-dependent. For instance, Boles et al. [24] conducted creep tests on a fully lithiated silicon nanowire (i.e., c-$Li_{3.75}Si$) at constant force levels, revealing a power-law creep behavior at stress levels approaching the yield strength of c-$Li_{3.75}Si$. Berla et al. [25] adopted the nanoindentation method to study the time-dependent mechanical behavior of lithiated silicon and found that lithiated silicon anodes creep readily under mechanical loadings. Pharr et al. [26] varied charging rates of silicon thin-film anodes while simultaneously measuring stresses. They observed that larger charging rates (i.e., strain rates) lead to higher stresses, which is indicative of a strong viscoplastic behavior of lithiated-silicon. Some potential mechanisms underpinning the viscoplasticity of lithiated silicon have been delineated. For example, Huang and Zhu [27] revealed that the high mobility of Li and the weak Li-Si bond facilitate continuous bond switching and accommodate plastic flow. Berla et al. [25] found the deformation of fully lithiatied silicon occurs by local and shear-driven rearrangement of small atomic clusters at the scale of $Li_{3.75}Si$. These processes take time and thus lead to the time-dependent viscoplastic behavior [26]. These studies underscore the importance of incorporating viscoplastic mechanical behavior into chemo-mechanical models to study the fully-coupled stress generation and lithiation reaction.

To decipher the coupling mechanism of mechanical stresses and lithiation reaction, investigation of the concurrent lithiation and deformation in lithiated silicon via chemo-mechanical modeling has attracted vast attention [28–32]. Lu et al. [33] proposed a modified Butler-Volmer equation by incorporating the stress effect into the activation energy and deciphered the phenomenon of voltage hysteresis due to mechanical stresses. Yin et al. [34] formulated a fully-coupled model of diffusion and stress generation, and investigated the diffusion-induced elastoplastic bending of bilayer electrodes. Yang et al. [35] developed a chemo-mechanical model in which lithium reaction is coupled with stress generation, and they modeled the morphology change of silicon nanowires during lithiation. Zhao et al. [14] identified the driving force of lithiation reaction at the interface and explicated the contribution of lithiation-induced stresses to the lithiation reaction. Zhang et al. [36] derived a stress-regulated interface velocity model for amorphous and crystalline silicon anodes by prescribing the evolution history of the mean stress at the interface. However, few efforts have been made to take the viscoplastic mechanical behavior of lithiated silicon into account to investigate how the lithiation of silicon proceeds in concert with viscoplasticity. A number of questions remain elusive. For example, what determines the velocity of the reaction interface (especially the initial interface velocity at the beginning of the lithiation)? How does the movement of reaction interface interact with the time-dependent viscoplastic behavior of the lithiated silicon? How is the stress generation affected by the coupling between reaction and deformation? Quantitative answers to these questions are crucial for understanding the fully-coupled lithiation reaction and stress generation in silicon anodes of lithium-ion batteries.

The purpose of this paper is to understand the coupling of stress generation and lithiation reaction in silicon anodes. To do so, we developed a chemo-mechanical model to study the lithiation process of a single silicon nanoparticle, from which the velocity of the reaction interface and the stress distribution in the silicon particle can be solved simultaneously via numerical methods. It is found that the interface velocity drops precipitously as the interface progresses into the particle because the viscoplastic deformation strongly counteracts the driving force of lithiation reaction. The predicted results of the interface position by our model are in line with the experimental measurements made by McDowell et al. [12]. Moreover, it is revealed that the lithiation-induced stresses depend on the interface velocity and thus are significantly mitigated by the slowing of the reaction interface. These results may provide important insight into the fully coupled stress generation and lithiation kinetics in silicon anodes of lithium-ion batteries.

## 2 A coupled chemo-mechanical model

### 2.1 Lithiation-reaction-induced stresses

This section outlines a mechanistic model we developed to explicate the stress generation under concurrent viscoplasticity and two-phase lithiation. We study a spherical crystalline silicon particle with an initial radius $B$ at the pristine

reference state, as illustrated in Figure 1(a). Figure 1(b) sketches that, upon lithiation, there forms a reaction interface separating the unreacted pristine Si core and the fully lithiated $Li_{3.75}Si$ shell. The interface exhibits a thickness $w$ about 1 nm, as revealed by the *in situ* atomic-scale TEM imaging [10]. The interface consists of an intermediate $Li_\eta Si$ phase ($0 < \eta < 3.75$), with several lithium atoms enclosing a single silicon atom or Si-Si pair. As the local lithium concentration at the interface grows high, the group of Li atoms collectively weakens the Si-Si bonds and dissociates silicon atoms from the pristine silicon phase, giving rise to the formation of fully lithiated $Li_{3.75}Si$ phase. Figure 1(c) illustrates the lithiation reaction, $Li^+ + e^- + \frac{1}{x}Si = \frac{1}{x}Li_xSi$, which takes place at the interface. The lithiation of the Si particle advances by the inward migration of the interface, with its radius $A$ continuously decreasing at a speed of $\dot{A}$ until the end of lithiation. Lithium insertion causes an increase in the volume of the lithiated silicon phase. During lithiation, a material element labeled by initial radius $R$ in the reference state is moved to a new position $r(t)$ in the current state to accommodate the lithiation-induced volume expansion. In particular, the outer radius of the particle expands to $b(t)$ in the deformed configuration.

To study the viscoplastic deformation induced by lithiation, we study a shell of lithiated silicon between the interface $A$ and radius $r (r > A)$ in the deformed configuration. The total lithiation-induced deformation can be decomposed into the elastic deformation, the plastic deformation and the chemical (volumetric) deformation caused by lithiation reaction, i.e., $\mathbf{F} = \mathbf{F}^e\mathbf{F}^p\mathbf{F}^c$. Since the elastic strain is negligible compared to the large plastic and volumetric strains, we thus neglect elastic deformation in both phases by setting $\mathbf{F}^e = \mathbf{I}$. Then the pristine silicon is modeled as a rigid body and the lithiated silicon is taken to be a rigid-plastic material. As a consequence, the shell between $A$ and $r$ in the current configuration is lithiated and deformed from a pristine silicon shell between $A$ and $R$ in the reference state, where $r$ is related to $A$ and $R$ by $r = [A^3 + \beta(R^3 - A^3)]^{\frac{1}{3}}$. $\beta$ represents the volume expansion ratio defined as the volume of $Li_{3.75}Si$ divided by the volume of pristine silicon. The deformation kinematics of the lithiated silicon shell is described by the total deformation gradient tensor $\mathbf{F} = \langle \lambda_r, \lambda_\theta, \lambda_\theta \rangle$. The total volume change of the lithiated silicon shell is given by $\det(\mathbf{F}) = \lambda_r \lambda_\theta^2 = \beta$. Therefore, the hoop stretch and radial stretch in the $Li_{3.75}Si$ shell are given by $\lambda_\theta = \frac{r}{R}$ and $\lambda_r = \frac{R^2}{r^2}\beta$. Moreover, the lithiation-induced volume expansion is intrinsically isotropic with $\mathbf{F}^c = \left\langle \beta^{\frac{1}{3}}, \beta^{\frac{1}{3}}, \beta^{\frac{1}{3}} \right\rangle$. Consequently, the plastic deformation tensor is

$$\mathbf{F}^p = \mathbf{F}(\mathbf{F}^c)^{-1} = \left\langle \frac{R^2}{r^2}\beta^{\frac{2}{3}}, \frac{r}{R}\beta^{-\frac{1}{3}}, \frac{r}{R}\beta^{-\frac{1}{3}} \right\rangle.$$

To determine the stress distribution in the fully lithiated silicon shell, we adopt a power-law viscoplastic flow potential to describe the viscoplastic mechanical behavior of the lithiated silicon

$$G(\sigma_{\text{eff}}) = \frac{\sigma_Y \dot{d}}{m+1}\left(\frac{\sigma_{\text{eff}}}{\sigma_Y} - 1\right)^{m+1}, \tag{1}$$

where $\sigma_Y$ is the yield strength, $\dot{d}$ is the reciprocal of viscosity and $m$ is the stress exponent. $\sigma_{\text{eff}}$ represents the effective stress. The plastic stretch rate tensor $\mathbf{D}^p$ can be evaluated as $\mathbf{D}^p = \frac{\partial G(\sigma_{\text{eff}})}{\partial \mathbf{S}}$, where $\mathbf{S}$ is the deviatoric stress tensor, so that

$$\mathbf{D}^p = \text{sgn}(\sigma_r - \sigma_\theta)\dot{d}\left(\frac{\sigma_{\text{eff}}}{\sigma_Y} - 1\right)^m \left\langle 1, -\frac{1}{2}, -\frac{1}{2} \right\rangle, \tag{2}$$

where $\text{sgn}(x)$ denotes the sign function. Note that the plastic stretch rate tensor can also be evaluated based on its definition that

$$\begin{aligned}\mathbf{D}^p = \dot{\mathbf{F}}^p(\mathbf{F}^p)^{-1} &= \left\langle \frac{\dot{\lambda}_r^p}{\lambda_r^p}, \frac{\dot{\lambda}_\theta^p}{\lambda_\theta^p}, \frac{\dot{\lambda}_\theta^p}{\lambda_\theta^p} \right\rangle \\ &= \frac{2(\beta-1)A^2\dot{A}}{r^3}\left\langle 1, -\frac{1}{2}, -\frac{1}{2} \right\rangle,\end{aligned} \tag{3}$$

where $\dot{A}$ denotes the interface velocity, which takes a negative value since the interface radius $A$ keeps decreasing as lithiation progresses (the reaction interface has never been seen to retreat during lithiation). Combining eqs. (2) and (3) gives that $\frac{2(\beta-1)A^2\dot{A}}{r^3} = \text{sgn}(\sigma_r - \sigma_\theta)\dot{d}\left(\frac{\sigma_{\text{eff}}}{\sigma_Y} - 1\right)^m$. For the rigid-plastic $Li_{3.75}Si$ phase, the volume expansion ratio $\beta = 4$ and $\sigma_{\text{eff}} \geq \sigma_Y$. It concludes that $\sigma_r - \sigma_\theta$ takes a negative sign and can be obtained as

$$\frac{\sigma_r - \sigma_\theta}{\sigma_Y} = -\left(\frac{\left[2(\beta-1)A^2\left|\dot{A}\right|\right]^n}{\dot{d}^n r^{3n}} + 1\right). \tag{4}$$

We use $n = 1/m$ to keep eq. (4) concise. The force balance at a material element located at radius $r$ requires that $\frac{\partial \sigma_r(r,t)}{\partial r} = 2\frac{\sigma_\theta(r,t) - \sigma_r(r,t)}{r}$. Plugging eq. (4) into the equilibrium equation and considering the traction-free boundary condition at the particle outer surface $r = b = [A^3 + \beta(B^3 - A^3)]^{\frac{1}{3}}$ gives the stress distribution in the $Li_{3.75}Si$ shell ($A < r \leq b$)

$$\frac{\sigma_r}{\sigma_Y} = \frac{2}{3n}\left[2(\beta-1)\left(\frac{A}{b}\right)^2\frac{\left|\dot{A}\right|}{\dot{d}b}\right]^n\left[1 - \left(\frac{b}{r}\right)^{3n}\right] + 2\log\left(\frac{r}{b}\right), \tag{5}$$

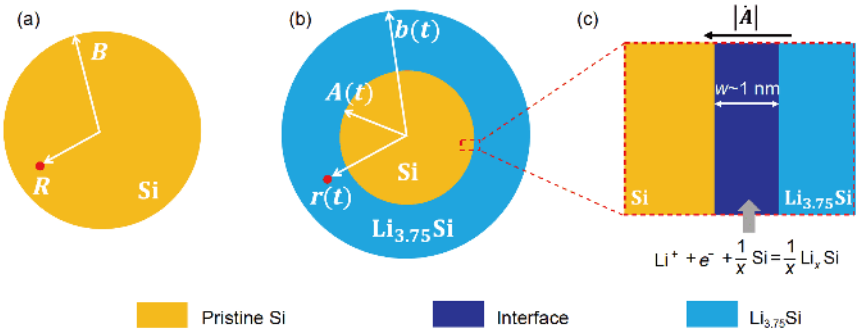


**Figure 1** (Color online) (a) In the reference state, a silicon nanoparticle anode exhibits an initial radius of $B$ (we only sketch the cross-section). A representative material element at a radius of $R$ is labeled by the red dot; (b) once lithiated, at time $t$, the element is deformed and pushed out to a new position of radius $r(t)$. The interface and the particle outer surface are identified by radii $A(t)$ and $b(t)$, respectively; (c) the interface (dark blue) exhibits a velocity $|\dot{A}(t)|$ and a thickness of $w$ (~1 nm). Lithiation reaction $\mathrm{Li}^{+}+e^{-}+\frac{1}{x}\mathrm{Si}=\frac{1}{x}\mathrm{Li}_{x}\mathrm{Si}$ takes place at the interface, causing the migration of the interface toward the particle center.

$$\frac{\sigma_\theta}{\sigma_{\mathrm{Y}}}=\left[2(\beta-1)\left(\frac{A}{b}\right)^2\frac{|\dot{A}|}{\dot{b}b}\right]^n\left[\frac{2}{3n}+\left(1-\frac{2}{3n}\right)\left(\frac{b}{r}\right)^{3n}\right]+2\log\left(\frac{r}{b}\right)+1. \tag{6}$$

Eqs. (5) and (6) indicate that the lithiation-induced stresses in the lithiated shell depend on both the interface radius $A$ and the interface velocity $\dot{A}$. By setting $|\dot{A}|=0$ in eqs. (5) and (6), we can obtain the stress distribution given in previous studies where lithiated silicon is postulated to be a rate-independent plastic material [14]. In their work, the stress distribution in the lithiated shell is dictated by the interface position $A$.

We next evaluate the stresses acting on the material element on the reaction interface. Hoop stretches at the interface are constrained by the inner rigid core so that $\mathbf{F}=\langle\beta,1,1\rangle$. The associated plastic deformation gradient tensor is thus given by $\mathbf{F}^{\mathrm{P}}=\left\langle\beta^{\frac{2}{3}},\beta^{-\frac{1}{3}},\beta^{-\frac{1}{3}}\right\rangle$. Lithiation of the reaction interface proceeds by the continuous insertion of lithium atoms into the atomically-thick interface layer, so that the volume expansion ratio $\beta$ at the interface increases at a rate of $\dot{\beta}(>0)$ until the interface is fully lithiated. We can derive the plastic stretch rate tensor of the form

$$\mathbf{D}^{p}=\dot{\mathbf{F}}^{p}\left(\mathbf{F}^{p}\right)^{-1}=\frac{2}{3}\frac{\dot{\beta}}{\beta}\left\langle 1,-\frac{1}{2},-\frac{1}{2}\right\rangle. \tag{7}$$

Comparing eqs. (7) and (2) yields that $\frac{2}{3}\frac{\dot{\beta}}{\beta}=\mathrm{sgn}(\sigma_r-\sigma_\theta)\dot{d}\left(\frac{\sigma_{\mathrm{eff}}}{\sigma_{\mathrm{Y}}}-1\right)^m$, indicating that $\sigma_r>\sigma_\theta$.

By assuming $\dot{\beta}$ is a constant on the interface, we adopt a simple lithiation kinetics model which relates the interface velocity $|\dot{A}|$ to $\dot{\beta}$ as [37]

$$|\dot{A}|=w/\left(\frac{\beta-1}{\dot{\beta}}\right)=w/\left(\frac{\beta-1}{\beta}\frac{\beta}{\dot{\beta}}\right). \tag{8}$$

To this end, the stress state on the interface can also be linked to the interface velocity $|\dot{A}|$ by $\frac{2(\beta-1)}{3\beta}\frac{|\dot{A}|}{w}=\mathrm{sgn}(\sigma_r-\sigma_\theta)\dot{d}\left(\frac{\sigma_{\mathrm{eff}}}{\sigma_{\mathrm{Y}}}-1\right)^m$, so that

$$\frac{\sigma_r-\sigma_\theta}{\sigma_{\mathrm{Y}}}=\left[\left(\frac{2(\beta-1)}{3\beta}\frac{|\dot{A}|}{\dot{w}w}\right)^n+1\right]. \tag{9}$$

The requirement that the radial stress should remain continuous across the interface gives the radial stress on the interface ($r$=$A$).

$$\frac{\sigma_r}{\sigma_{\mathrm{Y}}}=\frac{2}{3n}\left[2(\beta-1)\left(\frac{A}{b}\right)^2\frac{|\dot{A}|}{\dot{b}b}\right]^n\left[1-\left(\frac{b}{A}\right)^{3n}\right]+2\log\left(\frac{A}{b}\right). \tag{10}$$

Then the hoop stress on the interface can be solved by substituting eq. (10) into eq. (9)

$$\frac{\sigma_\theta}{\sigma_{\mathrm{Y}}}=\frac{2}{3n}\left[2\left(\beta-1\right)\left(\frac{A}{b}\right)^2\frac{|\dot{A}|}{\dot{b}b}\right]^n\left[1-\left(\frac{b}{A}\right)^{3n}\right]+2\log\left(\frac{A}{b}\right)-\left(\frac{2(\beta-1)}{3\beta}\frac{|\dot{A}|}{\dot{w}w}\right)^n-1. \tag{11}$$

Regarding the stress state in the rigid unlithiated silicon core, since the core is in a state of hydrostatic compression, the radial and hoop stresses are given by

$$\frac{\sigma_r}{\sigma_{\mathrm{Y}}}=\frac{\sigma_\theta}{\sigma_{\mathrm{Y}}}=\frac{2}{3n}\left[2(\beta-1)\left(\frac{A}{b}\right)^2\frac{|\dot{A}|}{\dot{b}b}\right]^n\left[1-\left(\frac{b}{A}\right)^{3n}\right]+2\log\left(\frac{A}{b}\right). \tag{12}$$

The lithiation-induced stress field within the silicon nanoparticle anode is fully specified by eqs. (5), (6), (10) and (12). The lithiation-induced stresses depend on the lithiation

process through two variables: the reaction interface position $A$ and the interface velocity $|\dot{A}|$. $|\dot{A}|$ and $A$ need to be obtained by considering the lithiation kinetics, which will be detailed in Sect. 2.2.

### 2.2 Stress-mediated lithiation reaction

Lithiation reaction takes place at the interface by transforming lithium ions, electrons, and silicon atoms into a lithiated silicon phase. The reaction is described by the chemical reaction equation that

$$\mathrm{Li}^+ + e^- + \frac{1}{x}\mathrm{Si} = \frac{1}{x}\mathrm{Li}_x\mathrm{Si}. \tag{13}$$

We can define the driving force of the chemical reaction as the net change of the free energy during the reaction: the free energy of the products minus that of the reactants. The driving force of the reaction consists of three terms [14]

$$\Delta G = \Delta G_{\mathrm{chem}} + \Delta G_{\mathrm{elec}} + \Delta G_{\mathrm{mech}}, \tag{14}$$

where $\Delta G_{\mathrm{chem}}$ represents the intrinsic free energy change due to the chemical reaction without any applied voltage and stresses. $\Delta G_{\mathrm{elec}}$ is the free energy change caused by the work done by the voltage, which is $-e\Phi$ ($\Phi$ is the applied voltage and $e$ the elementary charge). Herein, we would like to comment on the value of applied voltage $\Phi$ under different operating conditions. For the potentiostatic condition, $\Phi$ is apparently a constant. For the galvanostatic condition, Pharr et al. [38] have demonstrated that $\Phi$ decreases with time for a diffusion-limited process, while $\Phi$ remains constant for a reaction-limited process such as the initial lithiation of pristine silicon discussed in this work. To this end, it can be concluded that, in the present paper, the applied voltage $\Phi$ does not change over time, regardless of the specific operating conditions. $\Delta G_{\mathrm{mech}}$ denotes the contribution of mechanical stresses to the driving force for lithiation reaction.

Given the definition of the driving force $\Delta G$, the lithiation reaction at the interface occurs when $\Delta G<0$, while the reaction halts if $\Delta G\geq 0$. Such a sign convention suggests that a negative $\Delta G_{\mathrm{mech}}$ promotes lithiation reaction while a positive value of $\Delta G_{\mathrm{mech}}$ retards the reaction. The conclusion also applies to $\Delta G_{\mathrm{elec}}$ and $\Delta G_{\mathrm{chem}}$. $\Delta G_{\mathrm{chem}}$ intrinsically takes a negative value, for instance, $\Delta G_{\mathrm{chem}}=-0.18$ eV for $\mathrm{Li}_{2.1}\mathrm{Si}$. $\Delta G_{\mathrm{elec}}=-e\Phi$ is also negative. The value and sign of $\Delta G_{\mathrm{mech}}$ need to be determined by solving the stress field.

As a quantitative index of the lithiation reaction, the interface velocity $|\dot{A}|$ depends on the driving force $\Delta G$ by

$$|\dot{A}| = v_0\left[\exp\left(-\frac{\Delta G}{kT}\right) - 1\right], \tag{15}$$

where $v_0$ is a model parameter, $k$ is the Boltzmann constant and $T$ is the temperature. Note that eq. (15) is only applicable for $\Delta G\leq 0$ because the interface velocity $|\dot{A}|$ cannot be smaller than zero. We set $|\dot{A}| = 0$ for $\Delta G>0$ to reflect the fact that a positive $\Delta G$ stalls the lithiation reaction. Eq. (15) indicates that a more negative $\Delta G$ drives the interface to migrate at a higher velocity.

To determine the interface velocity $|\dot{A}|$, the contribution of mechanical stresses to the driving force for lithiation reaction needs to be identified. $\Delta G_{\mathrm{mech}}$ can be regarded as strain energy density stored on the interface (i.e., the products) minus the strain energy density stored in the unlithiated silicon core (i.e., the reactants). Thus we can evaluate $\Delta G_{\mathrm{mech}}$ by

$$\Delta G_{\mathrm{mech}} = \frac{1}{x}\left[\left(-\sigma_m^{\mathrm{Li}_x\mathrm{Si}}\Omega^{\mathrm{Li}_x\mathrm{Si}}\right) - \left(-\sigma_m^{\mathrm{Si}}\Omega^{\mathrm{Si}}\right)\right], \tag{16}$$

where $\Omega_m^{\mathrm{Si}}$ and $\Omega_m^{\mathrm{Li}_x\mathrm{Si}}$ represent the atomic volumes of Si and $\mathrm{Li}_x\mathrm{Si}$, respectively. $\sigma_m^{\mathrm{Si}}$ and $\sigma_m^{\mathrm{Li}_x\mathrm{Si}}$ denote the mean stress ($\sigma_m = \frac{\sigma_r + 2\sigma_\theta}{3}$) in the unlithiated silicon core and the mean stress on the reaction interface, respectively.

Plugging eqs. (14) and (16) in eq. (15) yields a relation between the interface velocity and the lithiation-induced stresses

$$|\dot{A}| = v_0\left[\exp\left(-\frac{\Delta G_{\mathrm{chem}} + \Delta G_{\mathrm{elec}} + \frac{1}{x}\left(\sigma_m^{\mathrm{Si}}\Omega^{\mathrm{Si}} - \sigma_m^{\mathrm{Li}_x\mathrm{Si}}\Omega^{\mathrm{Li}_x\mathrm{Si}}\right)}{kT}\right) - 1\right], \tag{17}$$

where $\sigma_m^{\mathrm{Si}}$ and $\sigma_m^{\mathrm{Li}_x\mathrm{Si}}$ can be evaluated by the stress distribution given in eqs. (10)–(12). Since the lithiation stresses in eqs. (10)–(12) depend on the interface position $A$ and the interface velocity $|\dot{A}|$, eq. (17) is an implicit nonlinear algebraic equation of $|\dot{A}|$ for a given $A$. Suppose the interface position $A(t)$ is known at time $t$, as abovementioned, eq. (17) becomes a nonlinear algebraic equation enabling one to numerically determine the interface velocity $|\dot{A}(t)|$ using the Newton-Raphson method. We should note that the initial condition for interface position $A(t)$ is given by $A(t=0) = B$, since the interface is right on the particle surface when the lithiation process sets in. Details about solving eq. (17) via the Newton-Raphson method are given in the Appendix. It follows that the stress fields in the lithiated silicon particle can be calculated by substituting $|\dot{A}(t)|$ and $A(t)$ into eqs. (5), (6) and eqs. (10)–(12), thereby accomplishing one loop of the numerical iteration. At the time $t+\Delta t$, the interface position $A$ is updated by the forward Euler method that $A(t+\Delta t) = A(t) - |\dot{A}(t)|\Delta t$, and the interface velocity $|\dot{A}(t+\Delta t)|$ and stress distribution can be determined by using the above scheme. In this way, one can determine the history of interface movement (i.e., the interface velocity $|\dot{A}(t)|$ as well as the interface position $A(t)$) and the stress distribution profiles iteratively.

## 3 Results and discussion

In this section, we employ the chemo-mechanical model described in Sect. 2 to study the coupled lithiation reaction and stress generation in the spherical lithiated silicon anode. To solve the interface migration and stress distribution, the following values are adopted: $\beta$=4, $\sigma_Y$=1 GPa, $\dot{d}$=0.002 [37], $n$=0.25 [37], $w$=1 nm [10], $B$=45 nm, $\Delta G_{chem}$=–0.18 eV [14], $x$=3.75, $\Phi$=0.42 V, $\Omega^{Si}$=2.0×10$^{-29}$ m$^3$ [14], $\Omega^{Li_{3.75}Si} = \beta\Omega^{Si}$= 8.0×10$^{-29}$ m$^3$, and $v_0$=0.163 nm/s [38]. The time increment $\Delta t$ adopted to iteratively update the interface position $A(t)$ is set to be 0.1 s. Results on coupled lithiation and stress generation are presented below.

### 3.1 Interface velocity and interface position

To understand how the viscoplastic stresses affect the interface migration, we plot the contribution due to mechanical stresses $\Delta G_{mech}$ in Figure 2 as a function of time $t$. It is found that the $\Delta G_{mech}$ initially equals to ~0.53 eV and increases monotonically with increasing time. It indicates that during lithiation of Si particle $\Delta G_{mech}$ is positive and thus retards the lithiation reaction, and the retardation effect becomes increasingly significant as the lithiation progresses. Recall that the total driving force $\Delta G$ for lithiation reaction is defined by $\Delta G$=$\Delta G_{chem}$–$e\Phi$+$\Delta G_{mech}$, and thus the condition for the lithiation reaction to occur is that $\Delta G \le 0$, i.e., $\Delta G_{mech} \le e\Phi - \Delta G_{chem}$=0.6 eV for our numerical example. Once $\Delta G_{mech}$ reaches 0.6 eV, the mechanical stresses are large enough to override the electrochemical driving force and thus stop the reaction at the interface. Figure 2 shows that $\Delta G_{mech}$ asymptotically approaches the critical value as time increases, gradually slowing down the lithiation reaction (i.e., reducing the velocity of the interface).

The obtained interface velocity $|\dot{A}(t)|$ is plotted in Figure 3 (a). The initial interface velocity is about 2.4 nm/s. McDowell et al. [12] conducted *in situ* TEM experiments of the lithiation of crystalline Si nanoparticles. They measured both the interface position and interface velocity vs time within each Si nanoparticle. The experimentally measured initial velocity of the interface is between 0.07 and 3 nm/s. Velocity calculated in our numerical example falls in the range. Considering the wide variation of factors in the experiments, including the electronic resistance of the substrate that the Si anodes are attached to and the ionic resistance at the solid electrolyte interface [12], our results on the initial velocity agree with the experimental measurement reasonably well. Moreover, in Figure 3(a), the interface velocity is seen to drop steeply as time increases. As shown in the inset of Figure 3(a), the interface velocity drops to 0.465 nm/s at $t$= 5 s (green line) and 0.106 nm/s at $t$=40 s (red line), with only 19.36% and 4.43% of the initial velocity remained. The results are in line with the experimental observation that the particles first undergo a rapid decrease in the core diameter followed by slowing of the reaction interface. The quick decrease of the interface velocity is a consequence of the interplay between viscoplasticity and the interface migration, which will be explained as follows. During coupled lithiation reaction and stress generation, the lithiation-induced stresses in the silicon particle are strain-rate-sensitive: the faster the interface velocity, the larger the lithiation-induced stresses, but not vice versa. As illustrated in Figure 3(a), the initial interface velocity is very high, leading to large mechanical stresses (as indicated by eqs. (5), (6), (10) and (12)). Large stresses result in high resistance to lithiation reaction (i.e., a more positive $\Delta G_{mech}$), thereby causing the rapid decrease of the interface velocity. To reveal the particle size effect on the interface velocity, we model silicon particles with various radii of $B$=40, 10, 45 and 100 nm, respectively. The results are summarized in Figure 3(b). As revealed by our previous work [37], larger particles undergo lower lithiation-induced stress, thereby giving rise to smaller resistance to lithiation reaction (i.e., reduced $\Delta G_{mech}$) at the interface. Consequently, the larger the particle radius, the higher the velocity of interface and the lithiation rate, as evident in Figure 3(b).

For ease of comparison between our results and experimental measurements in ref. [12], we sketch the interface diameter as a function of time in Figure 4. The interface diameter (i.e., the diameter of the unlithiated Si core, $2A(t)$) reduces with decreasing interface velocity (i.e., the slope of the curve) and end up a diameter about 43.4 nm at time $t$=500 s. The prediction from our model agrees well with the experimentally measured core diameter reported in ref. [12].

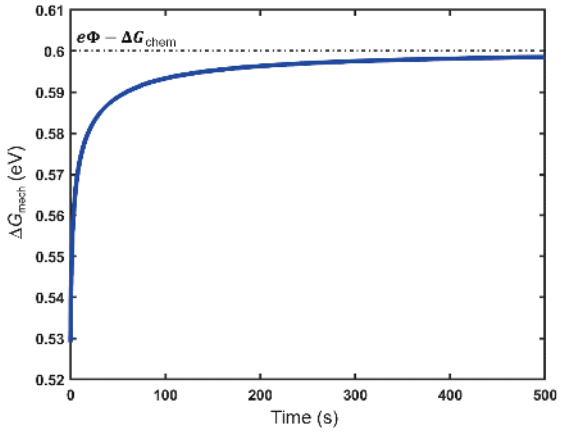


**Figure 2** (Color online) $\Delta G_{mech}$, the contribution of mechanical stresses to the driving force of the interfacial lithiation reaction ($Li^+ + e^- + \frac{1}{x}Si = \frac{1}{x}Li_xSi$), is sketched as a function of time. $\Delta G_{mech}$ acts as the resistance to the reaction and asymptotically approaches the critical value $e\Phi$–$\Delta G_{mech}$ which stalls the lithiation at the interface as well as the interface migration.

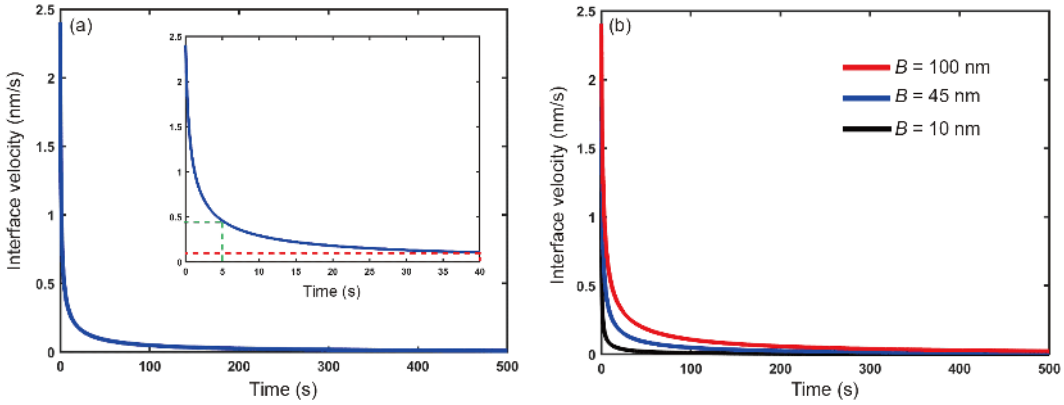


**Figure 3** (Color online) The interface velocity $|\dot{A}|$ is plotted as a function of time. (a) For particle radius $B$=45 nm, $|\dot{A}|$ shows an initial velocity about 2.4 nm/s and a precipitous decrease due to the coupled viscoplasticity and interface migration. The drop of velocity in the first 40 s of lithiation is shown in the figure inset. Interface velocity at $t$=5 and 40 s are highlighted by green and red dashed lines to quantitatively demonstrate the rapid velocity drop; (b) effect of particle radius on the interface velocity.

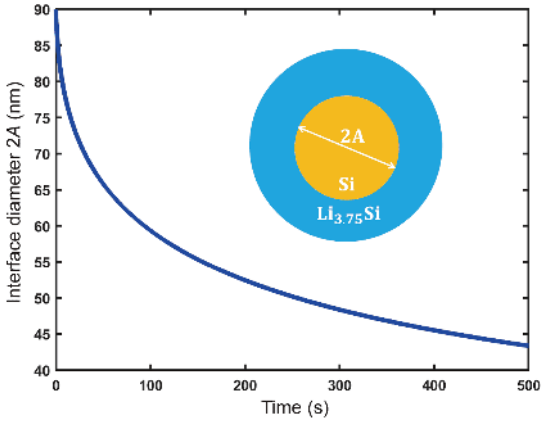


**Figure 4** (Color online) The interface diameter of $2A(t)$ is sketched over time. The curve shows an initial rapid decrease in the silicon core diameter, followed by a slowing of the reaction interface. The prediction agrees well with experimentally measured data reported in ref. [12].

### 3.2 Lithiation-reaction-induced stresses

Figure 5 sketches the lithiation-induced stress field in the reference state. The predicted radial stress $\sigma_r$ and the hoop stress $\sigma_\theta$ at time $t$=10 s are plotted as the blue lines in Figure 5 (a) and (b), respectively. The calculated interface radius $A$ is 38.9 nm (so that $\frac{A}{B}=0.864$) and the interface velocity $|\dot{A}|=0.295$ nm/s. To explicate the effect of lithiation process on the stress generation, results of two control studies with different values of $|\dot{A}|$ are included for comparison. Case No.1: the interface velocity is assumed to be independent of the lithiation-induced stress so that the interface velocity $|\dot{A}|$ remains to be the initial velocity $|\dot{A}|=2.4$ nm/s. Corresponding stress field is represented by the thin red line in Figure 5. Case No.2: the lithiated silicon is postulated to be a rate-independent plastic material. Consequently, the stress distribution does not depend on the interface velocity value and thus can be obtained by setting $|\dot{A}|\to 0$ nm/s in eqs. (5), (6), (10), and (12).

First, we should note that the hoop stress curves in Figure 5 (b) and (d) feature a discontinuous jump across the interface, which stems from the neglect of elastic strain as discussed in Sect. 2.1. Such discontinuity is intrinsic to the rigid-plastic behavior of lithiated silicon adopted in this work and has also been reported elsewhere [14]. Moreover, Comparing the predicted stress fields (blue line) with the Case No.1 (red line) shows that the stress-regulated lithiation is a "smart" process which helps protect the Si anodes by reducing the stress values: the lithiation reaction at the interface senses the reduced driving force due to the high stress level and reduces the interface velocity $|\dot{A}|$ accordingly. We further compare the predicted stress fields to the Case No.2 (black line), it is evident that taking lithiated silicon as a rate-independent plastic material underestimates the lithiation-induced stresses. In fact, at a given interface radius $A$, the obtained rate-independent stress field is the lower limit of the lithiation-induced stresses in viscoplastic lithiated silicon. To further reveal the evolution of the stress field, we plot the predicted radial stress $\sigma_r$ and the hoop stress $\sigma_\theta$ at time $t$=300 s as the blue line in Figure 5(c) and (d), respectively. The corresponding interface position $A$ and the interface velocity $|\dot{A}|$ are 24.19 nm ($\frac{A}{B}$=0.538) and $|\dot{A}|$=0.0166 nm/s, respectively. The comparison between the three cases indicates that, as the lithiation advances, the stresses in lithiated silicon particle gradually approach the rate-independent lithiated stress, indicating that the lithiation process helps reduce the lithiation-induced stresses.

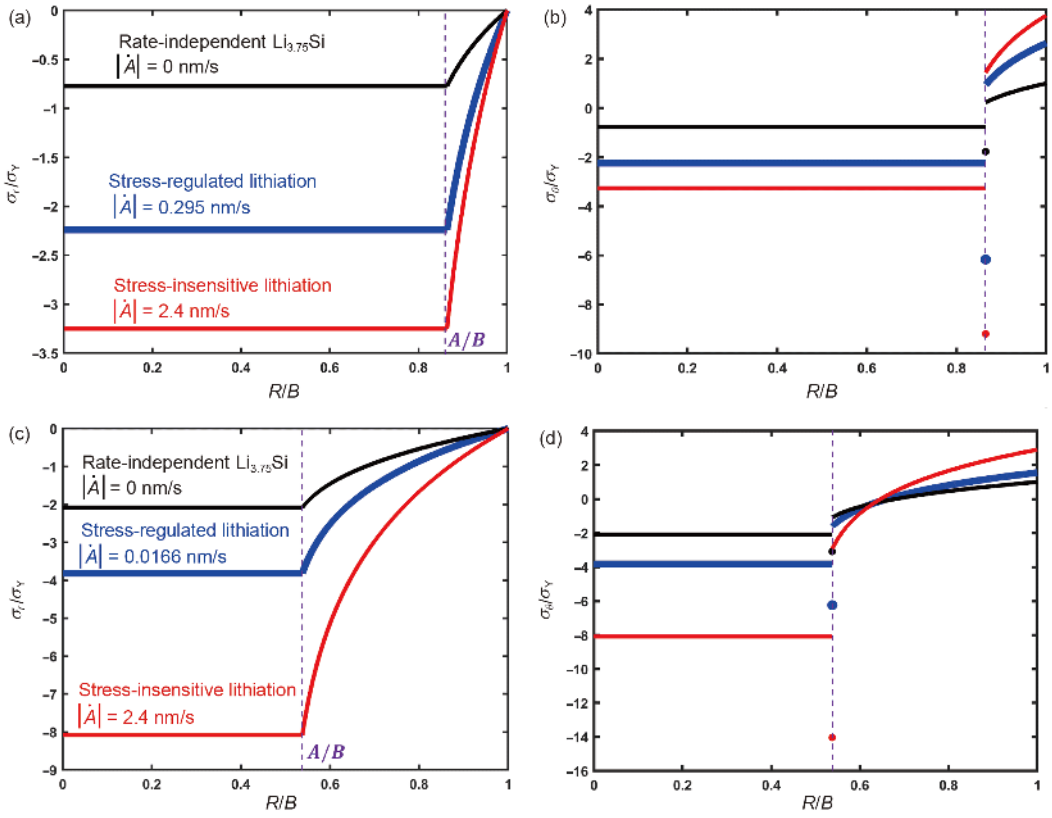


**Figure 5** (Color online) Lithiation-induced stress field is plotted in the reference state. At time $t$=10 s, the predicted radial stress $\sigma_r$ and the hoop stress $\sigma_\theta$ are shown as the blue lines in (a) and (b), respectively. Results of two control studies are also included. Case No.1 (red line): when the lithiation reaction is assumed to be stress-insensitive, the interface velocity remains to be a constant, the resulting stresses are of larger amplitude. Case No.2 (black line): if the lithiated silicon is considered to be a rate-independent material, the stresses can be obtained by setting $|\dot{A}| = 0$ and they set the theoretical lower limit for the lithiation-induced stresses under viscoplastic deformation. Stresses at time $t$=300 s are sketched in (c) and (d). Interface position is highlighted by the purple dashed lines.

### 3.3 Effect of reaction-deformation coupling

The coupling effect between lithiation reaction and stress generation can be summarized as follows.

The two processes are fully coupled: the lithiation-induced stress field at time $t$ in lithiated silicon is dependent on the interface position $A$ and the interface velocity $|\dot{A}|$. On the other hand, the interface velocity $|\dot{A}|$ is dictated by the lithiation-induced stresses across the reaction interface. It indicates that, for a given interface radius $A$, the stress field and the interface velocity are fully coupled and need to be solved simultaneously.

The stress-regulated interface migration acts as a stress-reducing mechanism: for a given interface radius $A$, the higher the interface velocity $|\dot{A}|$ is, the larger the lithiation-induced stresses and the resistance to lithiation reaction are, thereby reducing the interface velocity $|\dot{A}|$ and also the lithiation-induced stresses. Such negative feedback mechanism of stress-regulated interface migration serves as a "brake" to reduce the migration velocity and help protect the Si anode from large mechanical stresses.

## 4 Conclusion

We conclude by a few remarks of the above findings. The analysis in the present study focus on the initial lithiation of silicon anodes. In other words, the lithiation reaction advances via the movement of a sharp interface which separates a fully lithiated silicon phase and a pristine silicon phase. *In situ* TEM observations have revealed that there exists no visible interface in the first delithiation and subsequent lithiation/delithiation cycles. In this sense, the conclusion reported in this work holds mainly for silicon anodes subjected to the first lithiation. Although severe capacity fading is usually associated with the first lithiation due to fracture and SEI formation, investigating the coupling between Li migration and viscoplastic deformation during first delithiation and subsequent cycling is of great significance and warrants future exploration [39].

Results of lithiation kinetics based on the interface model, eqs. (14) and (15), show reasonable agreement with experimental evidence. For example, the interface velocity and interface position shown in Figures 3 and 4 are consistent with measurements conducted on crystalline silicon [12].

Moreover, the interface model implies that the interface migrates in a constant velocity when the contribution from mechanical stresses is negligible. The prediction agrees with experimental observations on amorphous silicon that the interface velocity is almost a constant during lithiation [39]. McDowell et al. [39] attributed the phenomenon to the much less significant stresses developed in a-Si electrode than its crystalline counterpart. Still, we would like to emphasize that the lithiation is a complex process and the interface model adopted in this study may not fully reflect its intricate nature. To further the understanding of the dynamics of lithiation, more systematic models of interfacial reaction are needed.

In conclusion, we formulated a chemo-mechanical model considering the fully-coupled lithiation reaction and viscoplastic deformation in silicon nanoparticle anodes for lithium-ion batteries. The interface position $A$, the interface velocity $|\dot{A}|$, and the corresponding stress distribution $\sigma = \langle \sigma_r, \sigma_\theta, \sigma_\theta \rangle$ can be solved simultaneously by Newton-Raphson method and forward Euler method iteratively. It is worth noting that the interface velocity $|\dot{A}|$, especially the initial velocity at the beginning of lithiation, cannot be obtained in previous studies which neglect the viscoplastic behavior of the lithiated silicon. We first show that, as the lithiation proceeds, the interface velocity reduces due to increasing resistance induced by the mechanical stresses (i.e., $\Delta G_{\text{mech}}$). The predicted interface position as a function of time is well in line with experimental measurements reported by McDowell et al. [12]. Then we reveal that the lithiation-induced stresses are dependent on the interface velocity $|\dot{A}|$ and the interface position through three dimensionless groups: the normalized interface radius $\frac{A}{B}$, the normalized interface velocity with respect to particle radius $\frac{|\dot{A}|}{\dot{d}B}$ and the normalized interface velocity with respect to interface thickness $\frac{|\dot{A}|}{\dot{d}w}$. It is evident that higher interface velocity (i.e., higher charging rates) results in higher stresses, which agrees with experimental observations. Moreover, we discover a stress-reducing mechanism due to coupled lithiation and stress generation: the larger the mechanical stresses, the higher the resistance to lithiation, and the lower the interface velocity $|\dot{A}|$, which eventually reduces the mechanical stresses. Through such a negative feedback mechanism, the stress-regulated migration serves as a "brake" to reduce the interface velocity and thus the lithiation-induced stresses, protecting the Si anodes from being subjected to excessive stresses. This work may shed light on understanding the chemo-mechanical coupling phenomenon in not only silicon anodes of lithium-ion batteries but also other binary solids system which involves concurrent reaction and deformation.

## Appendix

We outline the numerical method adopted to solve the interface velocity $|\dot{A}|$. $|\dot{A}|$ is given by

$$|\dot{A}| = v_0\left[\exp\left(-\frac{\Delta G}{kT}\right) - 1\right]. \tag{a1}$$

$\Delta G$ is the driving force for the lithiation reaction. According to eqs. (14) and (16), we can obtain that

$$\Delta G = \Delta G_{\text{chem}} - e\,\Phi + \frac{\Omega_{\text{Si}}}{x}\left(\sigma_m^{\text{Si}} - \beta\sigma_m^{\text{Li}_x\text{Si}}\right). \tag{a2}$$

The mean stresses in the silicon core and on the reaction interface are

$$\sigma_m^{\text{Si}} = C\sigma_{\text{Y}}|\dot{A}|^n + 2\sigma_{\text{Y}}\log\left(\frac{A}{b}\right), \tag{a3}$$

$$\sigma_m^{\text{Li}_x\text{Si}} = C\sigma_{\text{Y}}|\dot{A}|^n + 2\sigma_{\text{Y}}\log\left(\frac{A}{b}\right) - \frac{2\sigma_{\text{Y}}}{3}\left(\frac{1}{2\dot{d}b}\right)^n |\dot{A}|^n - \frac{2}{3}\sigma_{\text{Y}}, \tag{a4}$$

where the coefficient $C$ represents

$$C = \frac{2}{3n}\left[2(\beta-1)\left(\frac{A}{b}\right)^2\frac{1}{\dot{d}b}\right]^n\left[1-\left(\frac{b}{A}\right)^{3n}\right]. \tag{a5}$$

Eq. (a1) is a nonlinear algebraic equation of $|\dot{A}|$, which can be solved by adopting Newton-Raphson method. We define a function that $f(|\dot{A}|) = |\dot{A}| - v_0\left[\exp\left(-\frac{\Delta G}{kT}\right) - 1\right]$, thereby eq. (a1) is equivalent to

$$f(|\dot{A}|) = 0. \tag{a6}$$

According to the Newton-Raphson method, if we assume $|\dot{A}|_n$ at the $n^{\text{th}}$ iteration is known, then at the $(n+1)^{\text{th}}$ iteration

$$|\dot{A}|_{n+1} = |\dot{A}|_n - \frac{f\left(|\dot{A}|\right)}{f'\left(|\dot{A}|\right)}. \tag{a7}$$

The calculation is converged when $\left||\dot{A}|_{n+1} - |\dot{A}|_n\right| \le \text{tol}$, where tol is the error tolerance. We use tol=$10^{-12}$ in our calculation. Note that $f'$ denotes $\frac{\mathrm{d}f}{\mathrm{d}|\dot{A}|}$. The explicit expression of $f'$ and relevant derivatives needed to evaluate $f'$ are listed as follows:

$$f'(|\dot{A}|) = 1 + \frac{v_0}{kT}\exp\left(-\frac{\Delta G}{kT}\right)\frac{\mathrm{d}\Delta G}{\mathrm{d}|\dot{A}|}, \tag{a8}$$

$$\frac{\mathrm{d}\Delta G}{\mathrm{d}|\dot{A}|} = \frac{\Omega_{\text{Si}}}{x}\left(\frac{\mathrm{d}\sigma_{\text{mean}}^{\text{Si}}}{\mathrm{d}|\dot{A}|} - \beta\frac{\mathrm{d}\sigma_{\text{mean}}^{\text{Li}_x\text{Si}}}{\mathrm{d}|\dot{A}|}\right), \tag{a9}$$

$$\frac{\mathrm{d}\sigma_{\mathrm{mean}}^{\mathrm{Si}}}{\mathrm{d}\left|\dot{A}\right|} = Cn\left|\dot{A}\right|^{n-1}, \tag{a10}$$

$$\frac{\mathrm{d}\sigma_{\mathrm{mean}}^{\mathrm{Li_xSi}}}{\mathrm{d}\left|\dot{A}\right|} = Cn\sigma_{\mathrm{Y}}\left|\dot{A}\right|^{n-1} - \frac{2\sigma_{\mathrm{Y}}}{3}\left(\frac{1}{2\dot{d}b}\right)^{n} n\left|\dot{A}\right|^{n-1}. \tag{a11}$$

The coefficient $C$ is defined by eq. (a5). It is worth noting that the value of $C$ is dictated by the interface position $A(t)$. Once $A(t)$ is updated, $C$ needs to be updated accordingly.

*This work was supported by the National Natural Science Foundation of China (Grant Nos. 11802269, 11525210 & 11621062). The authors acknowledge the Fundamental Research Funds for the Central Universities. Zheng Jia also acknowledges the financial support from the One-Hundred Talents Program of Zhejiang University.*

1 Armand M, Tarascon J M. Building better batteries. Nature, 2008, 451: 652–657
2 Chan C K, Peng H, Liu G, et al. High-performance lithium battery anodes using silicon nanowires. Nat Nanotech, 2008, 3: 31–35
3 Kasavajjula U, Wang C, Appleby A J. Nano- and bulk-silicon-based insertion anodes for lithium-ion secondary cells. J Power Sources, 2007, 163: 1003–1039
4 Liu X H, Zhong L, Huang S, et al. Size-dependent fracture of silicon nanoparticles during lithiation. ACS Nano, 2012, 6: 1522–1531
5 Li D, Wang Y, Hu J, et al. *In situ* measurement of mechanical property and stress evolution in a composite silicon electrode. J Power Sources, 2017, 366: 80–85
6 Zhang X, Song W L, Liu Z, et al. Geometric design of micron-sized crystalline silicon anodes through in situ observation of deformation and fracture behaviors. J Mater Chem A, 2017, 5: 12793–12802
7 Yang L, Chen H S, Jiang H, et al. Failure mechanisms of 2D silicon film anodes: *In situ* observations and simulations on crack evolution. Chem Commun, 2018, 54: 3997–4000
8 Zhao K, Cui Y. Understanding the role of mechanics in energy materials: A perspective. Extreme Mech Lett, 2016, 9: 347–352
9 McDowell M T, Xia S, Zhu T. The mechanics of large-volume-change transformations in high-capacity battery materials. Extreme Mech Lett, 2016, 9: 480–494
10 Liu X H, Wang J W, Huang S, et al. *In situ* atomic-scale imaging of electrochemical lithiation in silicon. Nat Nanotech, 2012, 7: 749–756
11 Liu X H, Zheng H, Zhong L, et al. Anisotropic swelling and fracture of silicon nanowires during lithiation. Nano Lett, 2011, 11: 3312–3318
12 McDowell M T, Ryu I, Lee S W, et al. Studying the kinetics of crystalline silicon nanoparticle lithiation with *in situ* transmission electron microscopy. Adv Mater, 2012, 24: 6034–6041
13 Liu X H, Fan F, Yang H, et al. Self-limiting lithiation in silicon nanowires. ACS Nano, 2013, 7: 1495–1503
14 Zhao K, Pharr M, Wan Q, et al. Concurrent reaction and plasticity during initial lithiation of crystalline silicon in lithium-ion batteries. J Electrochem Soc, 2012, 159: A238–A243
15 Yang H, Liang W, Guo X, et al. Strong kinetics-stress coupling in lithiation of Si and Ge anodes. Extreme Mech Lett, 2015, 2: 1–6
16 Jia Z, Li T. Stress-modulated driving force for lithiation reaction in hollow nano-anodes. J Power Sources, 2015, 275: 866–876
17 Lang J, Ding B, Zhu T, et al. Cycling of a lithium-ion battery with a silicon anode drives large mechanical actuation. Adv Mater, 2016, 28: 10236–10243
18 Zhang S, Zhao K, Zhu T, et al. Electrochemomechanical degradation of high-capacity battery electrode materials. Prog Mater Sci, 2017, 89: 479–521
19 Bucci G, Swamy T, Bishop S, et al. The effect of stress on battery-electrode capacity. J Electrochem Soc, 2017, 164: A645–A654
20 Ding B, Wu H, Xu Z, et al. Stress effects on lithiation in silicon. Nano Energy, 2017, 38: 486–493
21 Sethuraman V A, Chon M J, Shimshak M, et al. *In situ* measurements of stress evolution in silicon thin films during electrochemical lithiation and delithiation. J Power Sources, 2010, 195: 5062–5066
22 Chon M J, Sethuraman V A, McCormick A, et al. Real-time measurement of stress and damage evolution during initial lithiation of crystalline silicon. Phys Rev Lett, 2011, 107: 045503
23 Fan F, Huang S, Yang H, et al. Mechanical properties of amorphous $Li_x$ Si alloys: A reactive force field study. Model Simul Mater Sci Eng, 2013, 21: 074002
24 Boles S T, Thompson C V, Kraft O, et al. *In situ* tensile and creep testing of lithiated silicon nanowires. Appl Phys Lett, 2013, 103: 263906
25 Berla L A, Lee S W, Cui Y, et al. Mechanical behavior of electrochemically lithiated silicon. J Power Sources, 2015, 273: 41–51
26 Pharr M, Suo Z, Vlassak J J. Variation of stress with charging rate due to strain-rate sensitivity of silicon electrodes of Li-ion batteries. J Power Sources, 2014, 270: 569–575
27 Huang S, Zhu T. Atomistic mechanisms of lithium insertion in amorphous silicon. J Power Sources, 2011, 196: 3664–3668
28 Wen J, Wei Y, Cheng Y T. Stress evolution in elastic-plastic electrodes during electrochemical processes: A numerical method and its applications. J Mech Phys Solids, 2018, 116: 403–415
29 Jia Z, Li T. Intrinsic stress mitigation via elastic softening during two-step electrochemical lithiation of amorphous silicon. J Mech Phys Solids, 2016, 91: 278–290
30 Zhang X, Krischok A, Linder C. A variational framework to model diffusion induced large plastic deformation and phase field fracture during initial two-phase lithiation of silicon electrodes. Comput Methods Appl Mech Eng, 2016, 312: 51–77
31 Zuo P, Zhao Y P. Phase field modeling of lithium diffusion, finite deformation, stress evolution and crack propagation in lithium ion battery. Extreme Mech Lett, 2016, 9: 467–479
32 Cui Z, Gao F, Qu J. A finite deformation stress-dependent chemical potential and its applications to lithium ion batteries. J Mech Phys Solids, 2012, 60: 1280–1295
33 Lu B, Song Y, Zhang Q, et al. Voltage hysteresis of lithium ion batteries caused by mechanical stress. Phys Chem Chem Phys, 2016, 18: 4721–4727
34 Yin J, Shao X, Lu B, et al. Two-way coupled analysis of lithium diffusion and diffusion induced finite elastoplastic bending of bilayer electrodes in lithium-ion batteries. Appl Math Mech-Engl Ed, 2018, 39: 1567–1586
35 Yang H, Fan F, Liang W, et al. A chemo-mechanical model of lithiation in silicon. J Mech Phys Solids, 2014, 70: 349–361
36 Zhang X, Lee S W, Lee H W, et al. A reaction-controlled diffusion model for the lithiation of silicon in lithium-ion batteries. Extreme Mech Lett, 2015, 4: 61–75
37 Jia Z, Liu W K. Rate-dependent stress evolution in nanostructured Si anodes upon lithiation. Appl Phys Lett, 2016, 109: 163903
38 Pharr M, Zhao K, Wang X, et al. Kinetics of initial lithiation of crystalline silicon electrodes of lithium-ion batteries. Nano Lett, 2012, 12: 5039–5047
39 McDowell M T, Lee S W, Harris J T, et al. *In situ* TEM of two-phase lithiation of amorphous silicon nanospheres. Nano Lett, 2013, 13: 758–764